HHS Public Access

Author manuscript

Neuroimage. Author manuscript; available in PMC 2018 January 15.

Published in final edited form as:

Neuroimage. 2017 January 15; 145(Pt A): 96–106. doi:10.1016/j.neuroimage.2016.10.011.

Magnetoencephalographic and functional MRI connectomics in schizophrenia via intra- and inter-network connectivity

Jon M. Houck[a,*], **Mustafa S. Çetin**[a], **Andrew R. Mayer**[b], **Juan R. Bustillo**[c], **Julia Stephen**[b], **Cheryl Aine**[c], **Jose Cañive**[c], **Nora Perrone-Bizzozero**[c], **Robert J. Thoma**[c], **Matthew J. Brookes**[d], and **Vince D. Calhoun**[a]

[a]University of New Mexico, Mind Research Network

[b]Mind Research Network

[c]University of New Mexico

[d]University of Nottingham

Abstract

Examination of intrinsic functional connectivity using functional MRI (fMRI) has provided important findings regarding dysconnectivity in schizophrenia. Extending these results using a complementary neuroimaging modality, magnetoencephalography (MEG), we present the first direct comparison of functional connectivity between schizophrenia patients and controls, using these two modalities combined. We developed a novel MEG approach for estimation of networks using MEG that incorporates spatial independent component analysis (ICA) and pairwise correlations between independent component timecourses, to estimate intra- and intern-network connectivity. This analysis enables group-level inference and testing of between-group differences. Resting state MEG and fMRI data were acquired from a large sample of healthy controls (n=45) and schizophrenia patients (n=46). Group spatial ICA was performed on fMRI and MEG data to extract intrinsic fMRI and MEG networks and to compensate for signal leakage in MEG. Similar, but not identical spatial independent components were detected for MEG and fMRI. Analysis of functional network connectivity (FNC; i.e., pairwise correlations in network (ICA component) timecourses) revealed a differential between-modalities pattern, with greater connectivity among occipital networks in fMRI and among frontal networks in MEG. Most importantly, significant differences between controls and patients were observed in both modalities. MEG FNC results in particular indicated dysfunctional hyperconnectivity within frontal and temporal networks in patients, while in fMRI FNC was always greater for controls than for patients. This is the first study to apply group spatial ICA as an approach to leakage correction, and as such our results may be biased by spatial leakage effects. Results suggest that combining these two neuroimaging modalities reveals additional disease-relevant patterns of connectivity that were not detectable with fMRI or MEG alone.

[*]Corresponding author: Jon M. Houck, University of New Mexico. Center on Alcoholism, Substance Abuse, and Addictions. MSC11 6280. Albuquerque, NM 87106. jhouck@unm.edu.

Keywords

Schizophrenia; imaging; MEG; Functional connectivity; Resting state connectivity

1. Introduction

More than 2000 neuroimaging papers examining the human “resting state” have been published since the first fMRI study (Biswal et al., 1995; Calhoun et al., 2001; Raichle et al., 2001). Analysis of resting state data has yielded information across a wide range of topics including basic sensory processing (Shostak, 1968), tobacco and alcohol use (Brown, 1968), neurodegenerative diseases (Rosadini et al., 1974), and neuropsychiatric illnesses (Reeve et al., 1993). Resting state protocols are particularly advantageous for the study of disease states where patients may have difficulty responding or performing behavioral tasks due to compromised cognitive and/or physiological functions. Connectivity methods such as independent component analysis (ICA) are a set of powerful analysis techniques used to analyze resting brain activity. Such approaches are particularly relevant to disease states such as schizophrenia, in which dysfunctional connectivity (“dysconnectivity”) is hypothesized to underlie patient symptoms (Bullmore et al., 1997; Stephan et al., 2006). Because this dysconnectivity is thought to be driven by aberrant synaptic plasticity (Stephan et al., 2009), characterizing functional connectivity may be essential to understanding the disorder.

Group independent component analysis (gICA) is an effective means of interrogating functional dysconnectivity in schizophrenia (Calhoun and Adali, 2012). As typically applied to resting fMRI data, this technique identifies and reconstructs temporally-coherent, spatially-independent networks in groups of subjects (Calhoun et al., 2001), where “networks” are defined as components identified via ICA. Spatial independence facilitates the comparison of topographies, or maps, between groups, while the property of temporal coherence permits the assessment of interregional, connectivity between spatially independent networks. However, exclusive reliance on fMRI to generate such networks may limit inference on dysconnectivity: Whilst the blood oxygenation-level dependent (BOLD) response measured by fMRI allows high spatial resolution maps, it is limited by being an indirect and slow physiological signal (Bandettini et al., 1993; Kim et al., 1997). Neural oscillatory activity, which comprises rhythmic electrical activity in cell assemblies, is thought to underlie BOLD responses. This occurs in the ~1–900Hz band; such rapid electrical signals cannot be assessed using fMRI but can be measured directly by techniques such as magnetoencephalography (MEG; Cohen, 1968), a noninvasive neuroimaging technique used to infer the cortical current distribution via assessment of the induced extra-cranial magnetic fields. Measurement of resting state brain activity using both fMRI and MEG, within a common sample of subjects, combines the strengths of each modality by allowing comparison of haemodynamic and electrophysiological effects. In this way we provide significant insight into functional connectivity, with special relevance for the study of schizophrenia and similar conditions. Significant progress towards integrating MEG and fMRI has been made in the past decade. MEG inverse solutions such now permit functional connectivity analysis in the same brain space as fMRI (Brookes et al., 2005). This approach

has already been used to evaluate intrinsic connectivity networks (ICNs) in MEG in a similar way to that typically used in fMRI (Brookes et al., 2011b). Neural oscillations are implicated strongly in this approach and in particular, multiple studies (Brookes et al., 2011b; Luckhoo et al., 2012) have now shown that assessment of temporal correlation between the amplitude envelopes of oscillatory activity facilitates elucidation of distributed network structure that bears reasonable resemblance to fMRI.

The purpose of the present study is to use both fMRI and band limited envelope correlation metrics in MEG to interrogate functional connectivity in the resting state in a sample of healthy normal volunteers and schizophrenia patients. Using methods based on group spatial ICA, for the first time we estimate networks from both MEG and fMRI and compare and contrast the networks and findings from the two modalities, with the hypotheses that 1) Patients and controls would differ significantly on both MEG and fMRI measures of intra-network connectivity, called functional network connectivity (FNC), and 2) MEG and fMRI spatial maps would show substantial overlap.

2. Materials and Methods

2.1 Participants

This investigation combined existing data from 91 participants, 46 schizophrenia patients and 45 healthy controls. Informed consent was obtained from all participants according to institutional guidelines at the University of New Mexico Human Research Protections Office (HRPO). All participants were compensated for their participation. Patients with a diagnosis of schizophrenia or schizoaffective disorder were invited to participate. Each patient completed the Structured Clinical Interview for DSM-IV Axis I Disorders (First et al., 1997) for diagnostic confirmation and evaluation of co-morbidities. Patients with a history of neurological disorders including head trauma (loss of consciousness > 5 minutes), mental retardation, history of substance dependence, or active substance abuse (except for nicotine) within the past year were excluded, as were patients who were clinically unstable (e.g., in the previous month were discharged from the hospital or had any changes in their psychotropic medications). Stability was also monitored throughout the study to confirm that patients had no clinically meaningful symptom changes. All patients had a negative urine toxicology for drugs of abuse at the time of enrollment in the study. Patients were treated with a variety of antipsychotic medications. The doses of antipsychotic medications were converted to olanzapine equivalents (see Table 1: Gardner et al., 2010). Healthy controls were recruited from the same geographic location and completed the SCID – Non-Patient Edition to rule out Axis I conditions (First et al., 2002). Although patients and controls were not yoked, demographic characteristics including age, gender, and caregiver socio-economic status (Werner et al., 2007) were monitored throughout recruitment to ensure that both groups were of similar composition. There were no significant between-group differences on these measures (see Table 1), and results were largely unchanged when demographic characteristics were included as covariates. All participant smokers were instructed not to use tobacco during the two hours prior to each scan to minimize acute effects. This was confirmed via a breath carbon monoxide measure of less than 8 ppm. Each participant

completed resting MEG and MRI scans. Scans were collected in counterbalanced order, with a median time between scans of approximately 22 days.

2.2 fMRI Data Acquisition

All fMRI data were collected on a 3-Tesla Siemens Trio scanner with a 12-channel radio frequency coil. High-resolution T1-weighted structural images were acquired with a five-echo MPRAGE sequence with TE = 1.64, 3.5, 5.36, 7.22, 9.08 ms, TR = 2.53 s, TI = 1.2 s, flip angle = 7°, number of excitations = 1, slice thickness = 1 mm, field of view = 256 mm, resolution = 256×256. T2*-weighted functional images were acquired using a gradient-echo EPI sequence with TE = 29 ms, TR = 2 s, flip angle = 75°, slice thickness = 3.5 mm, slice gap = 1.05 mm, field of view 240 mm, matrix size = 64x64, voxel size = 3.75 mm×3.75 mm×4.55 mm. Resting-state scans consisted of 149 volumes per run.

2.3 fMRI Data Preprocessing

An automated preprocessing pipeline and neuroinformatics system developed at MRN (Scott et al., 2011) was used to preprocess the fMRI data. The first four volumes were discarded to remove T1 equilibration effects. Images were realigned and slice-timing correction was applied using the middle slice as the reference frame in the functional data pipeline. The data were then spatially normalized to the standard MNI space, resampled to 3×3× 3 mm voxels, and smoothed using a Gaussian kernel with a full-width at half-maximum (FWHM) of 10 mm. The preprocessed time series data were scaled to a mean of 100.

2.4 fMRI Group Spatial Independent Component Analysis (gsICA)

Following Allen et al. (Allen et al., 2012), we performed a subject-specific data reduction PCA retaining 100 principal components (PC). In order to use memory more efficiently, group data reduction was performed using an EM-based PCA algorithm and C = 75 PCs were retained. The infomax algorithm (cf. Erhardt et al., 2011) was used for gICA. It was performed using the GIFT Toolbox (http://mialab.mrn.org/software/gift/). This high model order ICA (number of components, C = 75) affords a number of advantages, including the ability to use the resulting FNC matrix to infer how components would group in the case of a lower-dimension estimation, as well as refined components that correspond to known anatomical and functional segmentation (Allen et al., 2011; Kiviniemi et al., 2009). In order to estimate the reliability of the decomposition, the Infomax ICA algorithm was applied repeatedly via ICASSO (Himberg and Hyvarinen, 2003) and resulting components were clustered. Subject-specific maps and timecourses were estimated using a back-reconstruction approach based on PCA compression and projection (Calhoun et al., 2001).

2.5 fMRI Feature Identification

To identify non-artifactual components that contain features associated with resting state networks a combination of two methods was used (Allen et al., 2012). In the first method we examined the power spectra with two criteria in mind: dynamic range and low frequency/high frequency ratio. Dynamic range refers to the difference between the peak power and minimum power at frequencies to the right of the peak in the power spectra. Low frequency to high frequency power ratio is the ratio of the integral of spectral power below 0.10 Hz to

the integral of power between 0.15 and 0.25 Hz. To verify the results, three expert reviewers evaluated the components for functional relevance. In this evaluation, if a component exhibited 1) peak activation in gray matter, 2) low spatial overlap with known vascular, ventricular, motion, and susceptibility artifacts, and 3) TCs dominated by low frequency fluctuations, it was classified as a non-artifactual component. Of the 75 components returned by the gICA, 39 were identified as BOLD-related component; see Fig. S1.

2.6 MEG data acquisition

MEG data were collected in a magnetically and electrically shielded room (VAC Series Ak3B, Vacuumschmelze GmbH) using a whole-cortex 306-channel MEG array (Elekta Neuromag™) at the Mind Research Network. Before positioning the participant in the MEG, four coils were affixed to the participant's head: two on the forehead and one behind each ear. These coils allow determination of the position of the participant's head relative to the position and orientation of the MEG sensors. Additional positioning data were collected using a 3D digitizer (Polhemus Fastrak) in order to permit co-localization of MEG activity with the anatomical MRI result for each participant. Two channels of electro-oculogram (EOG), one vertical and one horizontal, and one channel of electrocardiogram (ECG) were collected simultaneously with MEG. MEG data were sampled at a rate of 1000 Hz, with a bandpass filter of 0.10 to 330 Hz. Head position was monitored continuously throughout the MEG session. Raw data were collected and stored. Participants were instructed to keep their eyes open and maintain fixation during the 6-minute scan to minimize occipital alpha rhythm (Cohen, 1968).

2.7 MEG data preprocessing

Artifact removal, correction for head movement, and downsampling to 250 Hz were conducted offline using Elekta Maxfilter software, with 123 basis vectors, a spatiotemporal buffer of 10 s, and a correlation limit of r=.95. Cardiac and blink artefacts were removed using a signal-space projection (SSP) approach (Uusitalo and Ilmoniemi, 1997). To facilitate an exploratory comparison with previous research (Brookes et al., 2011b), data were bandpass filtered into four frequency ranges of interest: delta (1–4 Hz), theta (5–9 Hz), alpha (10–15 Hz), and beta (16–29 Hz).

2.8 MEG beamformer projection

Covariance matrices were generated independently for each subject and frequency band, using all recorded data. Covariance matrices were regularized using a value of 4 times the minimum singular value of the unregularized matrix. That is, after estimation of the covariance matrix we regularized the matrix by adding a constant to the diagonal. The constant added was four times the minimum singular value of the unregularized covariance matrix. Voxels were placed on a regular 6-mm^3 grid spanning the brain image. Source orientation at each voxel was based on a nonlinear search for maximum projected signal-to-noise ratio. The forward solution was based on a dipole model (Sarvas, 1987) and a single-shell boundary element model (Hamalainen and Sarvas, 1989). Beamformer projection was performed separately for each subject and frequency range. After beamformer projection, source-space signals were normalized by an estimate of projected noise (Hall et al., 2013) and transformed to standard (MNI) space using FLIRT in FSL. A Hilbert transform was

applied to the time course at each voxel time to derive the analytic signal. The absolute value of this analytic signal was computed to yield the Hilbert envelope, an amplitude envelope of oscillatory power. The Hilbert envelope at each voxel was downsampled to an effective sampling rate of 1 Hz (Brookes et al., 2011b). Source space envelope data were smoothed spatially (6 mm^3 at full-width half-maximum), and the voxel size was resampled to 3×3×3 mm to facilitate comparison with the fMRI data. While strong and sustained correlations between brain regions can lead to beamformer failure, this requires correlations that persist through 30–40% of the period analyzed (Hadjipapas et al., 2005), unlikely in resting data (Brookes et al., 2011b).

2.9 MEG Group Spatial Independent Component Analysis (gsICA)

Group spatial ICA was applied to the individual subject data using the GIFT toolbox. The gsICA approach was selected over group temporal ICA (gtICA) for two reasons: 1) Because components produced by gsICA are not temporally independent, relations among network timecourses can be evaluated; and 2) gtICA of participant timecourses carries the assumption of temporal consistency, limiting its utility in group analysis of resting data. Replicating and extending the work of Brookes et al. (2011b), each frequency range was treated as a session in GIFT to permit exploratory analysis of each band, as well as the mean across bands. MEG ICA processing generally followed the procedures applied to the fMRI. Reduction steps were applied using principal component analysis. First, subject-specific data reduction was applied, retaining 100 principal components. Next, group level data reduction was applied to reduce the dataset to 75 principal components. Infomax ICA was applied 20 times in ICASSO and the resulting components were clustered. Spatial maps were generated by decomposing the mixed MEG timecourses to yield a set of spatially independent and temporally coherent networks. As with fMRI, subject-specific maps and timecourses were estimated using a back-reconstruction approach based on PCA compression and projection (Calhoun et al., 2001). This approach was chosen over alternate reconstruction approaches (e.g., GICA1, GICA2, dual regression) because it provides more accurate estimates for each subject and is more readily interpretable (Erhardt et al., 2011).

2.10 MEG feature identification

Consistent with standard practice (Allen et al., 2011; Robinson et al., 2009), component quality was assessed both qualitatively, to remove components situated in white matter and ventricles, and quantitatively, using assessments of dynamic range and the ratio of low-frequency to high-frequency power in each component. Components were separated into artifactual and non-artifactual components. Of the 75 components requested from the group ICA, 29 were retained as non-artifactual components; see Fig. S2. In the present context these criteria, originally applied previously to fMRI ICA components (Allen et al., 2011; Robinson et al., 2009), also appeared to perform well for MEG. As with fMRI, MEG FNC was defined as the zero-lag cross-correlations among reconstructed timecourses.

3. Results

3.1 Analytic approach

Resting MEG and fMRI data were acquired in 45 healthy controls and 46 schizophrenia patients. MEG data were source space projected using beamforming, enabling subsequent processing in brain space, equivalent to fMRI. Source space MEG and fMRI data were decomposed based upon a standard group spatial ICA analysis. This approach produces two forms of output: 1) network spatial maps and 2) network timecourses. Spatial maps reflect within-network connectivity (i.e., the extent to which the regions in a network tend to co-activate), while timecourses are used to assess among-network connectivity. For both MEG and fMRI, preprocessed timecourses were used to derive estimates of functional network connectivity (FNC) among networks, which we operationalized as pairwise zero-lag correlation between timecourses from spatially independent networks. Because the primary interest in the study was on commonalities in components across the frequency bands, analysis focused on the mean MEG, rather than on individual frequency bands.

3.2 Functional network connectivity (FNC)

We hypothesized that patients and controls would differ significantly on MEG and fMRI measures of FNC. FNC was assessed for each modality. Note that in MEG, we analysed FNC using a mean timecourse encompassing all frequencies, as this best reflects the commonalities in components across the frequency ranges examined. FNC coefficients were *z*-transformed prior to statistical analysis. Between-group differences in connectivity were evaluated using two-tailed *t*-tests, ascribing significance at $\alpha = .05$. We adjusted for multiple comparisons within each network matrix using the false discovery rate (FDR) correction. Significant FNC differences between patients and controls are shown in Fig. 1, projected onto a white matter surface in order to highlight the spatial pattern of among-network connectivity differences in the brain. This figure illustrates the spatial signature of the FNC differences observed between groups. Generally, we observed greater FNC in visual networks for fMRI components, and greater FNC in frontal networks for MEG components. Detailed FNC matrices for MEG and fMRI are presented in Fig. 2.

For fMRI, most group differences in intra-network connectivity were detected among temporal-occipital and frontal-occipital networks, and within the occipital networks (see Figs. 1, 2, and S3). For MEG, fewer FNC group differences were detected, with the majority in frontal-DMN networks and within the frontal networks. While fMRI FNC revealed no hyperconnectivity in SZ, approximately half of the MEG FNC relationships indicated higher connectivity in SZ than in HC, suggesting dysfunctional network connectivity in SZ networks revealed with MEG.

3.3 Spatial maps

We hypothesized that there would be considerable spatial overlap in network maps between MEG and fMRI. Spatial maps for each modality were assessed across groups via one-sample *t*-tests of back-reconstructed subject maps. Identified networks included temporal, sensorimotor, parietal, occipital, frontal, subcortical, and DMN regions (Fig. 3).

Commonalities and differences can be seen across participant groups for fMRI and MEG. Spatial overlap between MEG and fMRI was initially assessed via visual inspection and subsequently verified quantitatively using spatial correlation. In gsICA, the component map for the group is derived from the individual subject data, and is used to generate individual subject maps for that component via a back-reconstruction-process. Because examining spatial correlation using back-reconstructed subject maps would introduce circularity we instead used the group map, which represents the activity for that component across the whole group. Individual subject-level spatial correlation among these optimal matches ranged from 0.12 to 0.50, with a mean of 0.31. Point estimates and confidence intervals for these spatial correlations are reported in each panel of Fig. 4. Substantial overlap was detected across multiple networks including DMN as well as frontal, parietal, temporal, and occipital regions.

4. Discussion

The present study used an advanced data reduction approach, group ICA, to characterize patterns of brain connectivity in the resting state using MEG and fMRI in a sample of healthy volunteers and schizophrenia patients. Our results showed significant group differences in connectivity between these groups, with substantial spatial overlap as well as modality-specific patterns of functional network connectivity.

FNC group differences evident for MEG show greater functional connectivity across widespread frontal and temporal regions. Three interesting network patterns are seen in the MEG FNC results (Figs. 1 and S3). First, within the DMN we see that the dorsal anterior cingulate/superior frontal region appears hyperconnected for SZ compared to HC (blue regions) while posterior cingulate/precuneus is hypoconnected in SZ (red/orange regions). For HC, bilateral posterior cingulate is hyperconnected with an adjacent parietal component. Other recent studies of schizophrenia similarly showed hyperconnectivity within anterior cingulate for SZ (Jafri et al., 2008; Skudlarski et al., 2010). Hyperconnectivity has also been detected within one subcomponent of the DMN (i.e., anterior cingulate and portions of posterior cingulate) while the other subcomponent of the DMN revealed hypoconnectivity (bilateral parietal and dorsolateral prefrontal) for SZ (Skudlarski et al., 2010). These investigators identified the posterior cingulate as being the focus of decoupling found between anatomical (DTI) and functional (fMRI) connectivity. They emphasized that the DMN should not be viewed as a single unit; it is composed of substructures that all contribute to resting state activation but vary substantially in connectivity patterns.

The second interesting MEG result in Figs. 1 and 2 shows widespread hyperconnectivity between perisylvian and frontal regions which closely resemble that seen in fMRI resting state of SZ patients who reportedly experience auditory hallucinations (Diederen et al., 2013; Sommer et al., 2012). These regions include bilateral superior temporal gyri (i.e., auditory cortex) and middle temporal gyrus, along with supramarginal gyrus, and what appears as the right hemisphere homologue of Wernicke’s area (Jardri et al., 2010; Sommer et al., 2012). Stephen and colleagues (Stone et al., 2014) have been examining multisensory integration in SZ and find that SZ benefit from multisensory (auditory/visual) integration more than do HC. She has related these results to the “high noise” theory where increased

activity during rest has been attributed to impaired responsiveness to external stimuli. This widespread hyperconnectivity involving auditory and speech perception regions may provide important support for the “high noise” theory; this widespread network appears to be hyperconnected for SZ, compared to HC, during normal resting state. Therefore, additional stimulus intensity and/or additional attention resources may be required for SZ to direct their attention to the external environment. In support of this interpretation, the attentional parietal regions are hyperconnected in HC. These patterns of functional connectivity lead us to speculate that SZ are directed inward more during resting state while HC are directed toward the external environment, ready to respond. Altogether our results indicate that multimodal methods are essential to understanding the mechanisms of inter-regional brain connectivity. (cf. Brookes et al., 2011a).

Recent meta-analytic work on fMRI of the resting state in schizophrenia has revealed that schizophrenia patients tend to show hyperactivation bilaterally in lingual gyrus and broad hypoactivity elsewhere, with decreases in resting state activity observed in VMPFC, left hippocampus, PCC, and precuneus (Kühn and Gallinat, 2013). Other implicated regions with lower connectivity include paracingulate cortex, bilateral thalamus, fusiform, left caudate, and left thalamus(Argyelan et al., 2013), with greater hypoactivity generally related to worse functioning. Larger studies of functional network connectivity in schizophrenia have indicated dysfunction across a range of networks, with schizophrenia-specific deficits in midbrain/cerebellar and fronto-temporal paralimbic networks (Khadka et al., 2013). Our data suggest that patterns of connectivity involving hippocampus, fusiform, and middle frontal regions are particularly relevant to the level of functioning within the sample patient group, a finding consistent with the observed patient-control differences in frontal and temporal networks. Notably, each neuroimaging modality we examined contributed both common and unique findings.

Our exploratory MEG analysis of within-frequency FNC (Fig. S3) showed multiple group differences in inter-regional connectivity in the beta (16–29 Hz) range, particularly in the frontal-cerebellar, frontal-DMN, and frontal-auditory networks. Nearly all FNC group differences in the beta range suggested hyperconnectivity in patients. It is worth noting, however, that because this was an exploratory analysis separate FDR corrections were applied within each frequency band; the analysis of band-specific group differences was not subjected to an additional correction for multiple comparisons. These additional exploratory results should be viewed with some caution, pending replication. Beta band has previously been implicated in long-range cortical synchrony (Stein et al., 1999; Tallon-Baudry et al., 2004, 2004; Thatcher et al., 2008), notably in visual processing (Sehatpour et al., 2008) and working memory (Piantoni et al., in press) networks observed in the present data. Consistent with the present study, research in schizophrenia has indicated abnormal synchronization in the beta and gamma ranges (Uhlhaas and Singer, 2011, 2010), particularly in the beta band (Siebenhühner et al., 2013). Synchrony between the two hippocampi, regions with particular relevance for schizophrenia (Hanlon et al., 2012, 2011), has also been linked to the beta band (Lee et al., 2014).

What do we learn about functional connectivity in schizophrenia from this dual modality study? By combining both MEG and fMRI we are able to interrogate both network structure

(maps) and network dynamics (FNC) in schizophrenia, revealing patterns of connectivity impossible to detect with either modality alone. In particular, MEG appeared more sensitive to hyperconnectivity in frontal and temporal networks among patients. On the whole, our resting fMRI FNC findings converge with the schizophrenia literature, which reports hypoactivation across multiple regions, including the prefrontal cortex (Kühn and Gallinat, 2013). However, prefrontal FNC with MEG was increased in our patient group. This suggests abnormally increased synchronous firing from neuronal populations in prefrontal networks in these chronically ill schizophrenia patients. Whether these hyper-synchronous networks underlie core deficits of the illness or represent compensation to overcome other primary functional defects, we cannot say. However, we did not find correlations with positive symptoms, which have been reported to be associated with fMRI functional hyper-connectivity (Ford et al., 2014). Our results suggesting hyper-synchronous prefrontal networks are consistent with the dysconnectivity model of schizophrenia (Stephan et al., 2006) and suggest that these represent a deficit at the neuronal population level and not merely in the coupling of vascular/neuronal function.

In the present study, the combination of data from multiple modalities, collected at different times, conveys additional confidence in our results. For instance, one critique of resting fMRI data from populations with mental illness or disease is that patients may respond differentially to auditory scanner noise (Skouras et al., 2013). We observed bilateral temporal components in fMRI, which has substantial background noise during scans, and unilateral temporal components in MEG, which is silent, providing some support for this critique. Similarly, schizophrenia patients have well-known autonomic nervous system dysregulation (Bär et al., 2007; Rachow et al., 2011; Toichi et al., 1999) related to variability in heart rate and respiration (Paterson, 1935; Whitehorn and Richter, 1937; Wittkower, 1934) which can directly affect the BOLD response (Cohen et al., 2002). However, the electromagnetic signal detected by MEG is less affected, particularly when the cardiac signal has been removed as in the present study. Overlapping MEG-fMRI components can reasonably be assumed to be free of such influences, revealing only the underlying dysregulation. Finally, eye movements also differ between controls and patients (Clementz and Sweeney, 1990), again directly affecting the BOLD signal, where changes in the flow of vitreous humor during eye movement increase signal variance from nearby regions (Beauchamp, 2003). The corneo-retinal potential can affect electrophysiological signals (Kolder and North, 1966), but generally would appear as a source between the eyes. In the present study, such eye movement artifacts were reduced through the application of SSP. Surviving frontal and occipital components that are in common for MEG and fMRI are arguably free of such modality-specific artifacts.

Point spread – that is, the leakage of signal between projected timecourses – is a ubiquitous issue in beamformer analysis (Brookes et al., 2012; Colclough et al., 2015; Hipp et al., 2012; Palva and Palva, 2012). In connectivity analysis, signal leakage manifests as zero-lag correlation between timecourses of spatially separate regions. Connectivity analysis of beamformer-projected timecourses without leakage correction will therefore lead to spurious connectivity estimates if one simply computes the connectivity between two source signals. Because signal leakage varies with sensor geometry, brain region, sensor noise, inverse solution, and the sparseness of the source space, no universal correction for leakage exists.

The predominant approaches to correcting for leakage rely to some degree upon removing or ignoring zero-order correlations between timecourses. This includes partial correlation approaches, and, in phase-based connectivity, either analysis of the asymmetry of the phase distribution or removal of the real portion of coherence. Such approaches can be problematic because they discard true zero-order relationships, throwing out the signal 'baby' with the leakage 'bathwater'. Further, these approaches are problematic because they rely to varying degrees on the assumption that brain sources are point sources rather than distributed sources. However, research in intracranial EEG has demonstrated that cortical sources are often distributed over at least 10 cm^2 of the cortical surface (Chowdhury 2013, Huiskamp 2010) – that is, spatially-distributed sources detected via MEG may represent true distributed sources in the cortex. Therefore, even if an all-to-all voxelwise leakage correction were practical, it would be inadvisable, as it could broadly suppress true source extents (Jerbi et al., 2004)

Given this, group spatial independent component analysis (sICA) may eventually provide a preferable form of leakage correction for FNC-based studies. In this data-driven technique for unmixing complex brain signals (Calhoun et al., 2001), the unmixing procedure produces a set of maximally independent network topologies (i.e., component maps), with timecourses that may be inter-related. Relationships among these networks can then be evaluated, as in the present study, using functional network connectivity (FNC). The leakage of signal among MEG sensors typically manifests as linear spatial blurring of the sources (cf. Palva and Palva, 2012; Schoffelen and Gross, 2009; Wens, 2015). This blurring will inflate the connectivity among cross-correlated sensor signals, potentially producing spurious estimates of connectivity if not addressed. However, such a signal is well-suited to unmixing by sICA, and when present may manifest as a spatial blurring of each individual component. The connectivity *among* these components might be relatively less influenced by leakage in such a scenario, as the ICA unmixing procedure may be expected to capture both source and leakage within a single component, as both source and leakage are by definition quite highly related. In the present study, our approach and statistical testing is focused on the cross-correlation among gICA-derived timecourses and as such the effects of signal leakage on these estimates of connectivity might be expected to be low. However, such claims need to be directly evaluated, a task which is beyond the scope of the current work but which we are pursuing in a separate paper. Should this approach be supported in our follow-up work, it may ultimately prove inadvisable to perform a separate leakage correction step if one is testing gICA-based among-component connectivity, or FNC. However, given the novelty of this approach, we need to mention that it is possible that FNC results presented in the present study are biased to some extent by signal leakage. As such, they should be viewed with some caution pending replication.

Other approaches to leakage require additional considerations such as the rank of the data. MEG data is of relatively low rank, which is further reduced if signal space separation is applied (Taulu and Kajola, 2005). Some approaches to leakage correction (e.g., Colclough et al., 2015) require that the rank of the data is equal to or higher than the number of timecourses being corrected. Studies taking that approach must therefore be careful to use an appropriate number of basis vectors during signal space separation to ensure that the resulting data will have adequate rank for leakage correction.

4.1 Limitations

While the initial result of this innovative approach are promising, several caveats should be noted. First, although this study combined MEG and fMRI, data from each modality were collected and analyzed separately, albeit in parallel. Techniques for true whole-brain multi-modal data fusion remain elusive, and potential sources of inter-modality differences such as the day of the scan and time of the scan cannot be ruled out. Second, although substantial spatial overlap was observed for MEG and fMRI, there was minimal overlap in the patterns of connectivity (i.e., FNC) between MEG and fMRI. This may be due to some sample-specific idiosyncrasies, to the differing sensitivities of FNC analysis between the two modalities, or to some combination of these factors. The optimal approach to addressing these issues is via replication in similar samples, which we hope to pursue in a future study. Third, while multiple MEG frequency bands were examined, this portion of the analysis was exploratory in nature. Future work should examine between-group effects both within frequency and across frequencies, an approach that will require a larger sample to ensure adequate power to detect such effects. Fourth, the inversion of MEG data from measurement channels to brain sources is an ill-posed problem, with approximately 300 measurement channels in most commercial devices, but thousands of potential sources in the brain. Although sources with high signal-to-noise ratio (SNR) can be resolved with separation of 0.5 mm using a beamformer approach (Hillebrand and Barnes, 2005), lower SNR data such as that obtained in resting studies will typically lead to local blurring of source activity. Fifth, while the ICA decomposition assumes a linear relationship between the derived components and the source signal, the BOLD signal and MEG source envelopes analyzed in the present study are themselves nonlinear functions of the true source signals, and the extent to which the ICA accurately represents this nonlinearity is unclear. Finally, although the present study used spatial ICA as an approach to leakage correction, it may be the case that the ICA unmixing procedure does not adequately compensate for leakage. A detailed simulation study testing this approach, while beyond the scope of the present study, is now in process.

4.2 Conclusion

The present study employed a novel approach to estimate intrinsic connectivity networks from group spatial ICA of fMRI and MEG data to evaluate spatial patterns and functional connectivity in a sample of schizophrenia patients and healthy volunteers. This is the first study to use group spatial ICA with resting MEG data, and also the first to apply these methods to directly compare a patient population to healthy volunteers. We observed substantial spatial overlap in multiple intrinsic connectivity networks as assessed using spatial correlation. We also observed intermodality differences in functional network connectivity of ICNs, with more instances of high frontal FNC for MEG and high occipital FNC for fMRI. In addition, while group differences in network spatial topography were observed primarily in frontal regions for fMRI, in MEG these differences were observed more broadly in frontal and temporal networks. The results suggest hyper-synchronous prefrontal networks in schizophrenia with deficits at the neuronal population level and not merely in neurovascular coupling. The spatial consistency of components from MEG and fMRI, based on data collected on different days, also allows us to rule out several alternative explanations for the observed results, including modality-specific scanner and environmental

noise. Results suggest that the application of group spatial ICA to multimodal neuroimaging using MEG and fMRI provides important information about complex mental illnesses such as schizophrenia that would have been missed otherwise.

Supplementary Material

Refer to Web version on PubMed Central for supplementary material.

Acknowledgments

Research reported in this publication was supported by the National Institute for Research Resources, National Institute of General Medical Sciences, and National Institute on Alcohol Abuse and Alcoholism of the National Institutes of Health (NIH) under award numbers P20RR021938, P20GM103472, and K01AA021431. The content is solely the responsibility of the authors and does not necessarily represent the official view of the NIH.

References

Allen EA, Erhardt EB, Damaraju E, Gruner W, Segall JM, Silva RF, Havlicek M, Rachakonda S, Fries J, Kalyanam R, Michael AM, Caprihan A, Turner JA, Eichele T, Adelsheim S, Bryan AD, Bustillo J, Clark VP, Ewing SWF, Filbey F, Ford CC, Hutchison K, Jung RE, Kiehl KA, Kodituwakku P, Komesu YM, Mayer AR, Pearlson GD, Phillips JP, Sadek JR, Stevens M, Teuscher U, Thoma RJ, Calhoun VD. A baseline for the multivariate comparison of resting-state networks. Front. Syst. Neurosci. 2011; 5:1–23. [PubMed: 21347218]

Allen EA, Erhardt EB, Wei Y, Eichele T, Calhoun VD. Capturing inter-subject variability with group independent component analysis of fMRI data: A simulation study. NeuroImage. 2012; 59:4141–4159. [PubMed: 22019879]

Argyelan M, Ikuta T, DeRosse P, Braga RJ, Burdick KE, John M, Kingsley PB, Malhotra AK, Szeszko PR. Resting-State fMRI Connectivity Impairment in Schizophrenia and Bipolar Disorder. Schizophr. Bull. 2013:sbt092.

Bandettini PA, Jesmanowicz A, Wong EC, Hyde JS. Processing strategies for time-course data sets in functional MRI of the human brain. Magn. Reson. Med. Off. J. Soc. Magn. Reson. Med. Soc. Magn. Reson. Med. 1993; 30:161–173.

Bär K-J, Boettger MK, Koschke M, Schulz S, Chokka P, Yeragani VK, Voss A. Non-linear complexity measures of heart rate variability in acute schizophrenia. Clin. Neurophysiol. 2007; 118:2009–2015. [PubMed: 17646130]

Beauchamp MS. Detection of eye movements from fMRI data. Magn. Reson. Med. 2003; 49:376–380. [PubMed: 12541259]

Biswal B, Zerrin Yetkin F, Haughton VM, Hyde JS. Functional connectivity in the motor cortex of resting human brain using echo-planar mri. Magn. Reson. Med. 1995; 34:537–541. [PubMed: 8524021]

Brookes MJ, Gibson AM, Hall SD, Furlong PL, Barnes GR, Hillebrand A, Singh KD, Holliday IE, Francis ST, Morris PG. GLM-beamformer method demonstrates stationary field, alpha ERD and gamma ERS co-localisation with fMRI BOLD response in visual cortex. NeuroImage. 2005; 26:302–308. [PubMed: 15862231]

Brookes MJ, Hale JR, Zumer JM, Stevenson CM, Francis ST, Barnes GR, Owen JP, Morris PG, Nagarajan SS. Measuring functional connectivity using MEG: Methodology and comparison with fcMRI. NeuroImage. 2011a; 56:1082–1104. [PubMed: 21352925]

Brookes MJ, Woolrich M, Barnes GR. Measuring functional connectivity in MEG: A multivariate approach insensitive to linear source leakage. NeuroImage. 2012; 63:910–920. [PubMed: 22484306]

Brookes MJ, Woolrich M, Luckhoo H, Price D, Hale JR, Stephenson MC, Barnes GR, Smith SM, Morris PG. Investigating the electrophysiological basis of resting state networks using magnetoencephalography. Proc. Natl. Acad. Sci. 2011b

Brown BB. Some characteristic EEG differences between heavy smoker and non-smoker subjects. Neuropsychologia. 1968; 6:381–388.

Bullmore ET, Frangou S, Murray RM. The dysplastic net hypothesis: an integration of developmental and dysconnectivity theories of schizophrenia. Schizophr. Res. 1997; 28:143–156. [PubMed: 9468349]

Calhoun VD, Adali T. Multisubject Independent Component Analysis of fMRI: A Decade of Intrinsic Networks, Default Mode, and Neurodiagnostic Discovery. Biomed. Eng. IEEE Rev. In. 2012; 5:60–73.

Calhoun VD, Adali T, Pearlson GD, Pekar JJ. A method for making group inferences from functional MRI data using independent component analysis. Hum. Brain Mapp. 2001; 14:140–151. [PubMed: 11559959]

Clementz BA, Sweeney JA. Is eye movement dysfunction a biological marker for schizophrenia? A methodological review. Psychol. Bull. 1990; 108:77–92. [PubMed: 2200074]

Cohen D. Magnetoencephalography: Evidence of Magnetic Fields Produced by Alpha-Rhythm Currents. Science. 1968; 161:784–786. [PubMed: 5663803]

Cohen ER, Ugurbil K, Kim S-G. Effect of Basal Conditions on the Magnitude and Dynamics of the Blood Oxygenation Level–Dependent fMRI Response. J. Cereb. Blood Flow Metab. 2002; 22:1042–1053. [PubMed: 12218410]

Colclough GL, Brookes MJ, Smith SM, Woolrich MW. A symmetric multivariate leakage correction for MEG connectomes. NeuroImage. 2015; 117:439–448. [PubMed: 25862259]

Diederen KMJ, Neggers SFW, de Weijer AD, van Lutterveld R, Daalman K, Eickhoff SB, Clos M, Kahn RS, Sommer IEC. Aberrant resting-state connectivity in non-psychotic individuals with auditory hallucinations. Psychol. Med. 2013; 43:1685–1696. [PubMed: 23199762]

Erhardt EB, Rachakonda S, Bedrick EJ, Allen EA, Adali T, Calhoun VD. Comparison of multi-subject ICA methods for analysis of fMRI data. Hum. Brain Mapp. 2011; 32:2075–2095. [PubMed: 21162045]

First, M.; Spitzer, R.; Gibbon, M.; Williams, J. Structured clinical interview for DSM-IV axis I disorders-clinician version (SCID-CV). Wash. DC: Am. Psychiatr. Assoc. Press; 1997.

First MB, Spitzer RL, Gibbon M, Williams JB. Structured clinical interview for DSM-IV-TR axis I disorders, research version, Non-patient edition. SCID-I/P. 2002

Ford JM, Palzes VA, Roach BJ, Potkin SG, Erp TGMvan, Turner JA, Mueller BA, Calhoun VD, Voyvodic J, Belger A, Bustillo J, Vaidya JG, Preda A, McEwen SC, Mathalon DH. Visual Hallucinations Are Associated With Hyperconnectivity Between the Amygdala and Visual Cortex in People With a Diagnosis of Schizophrenia. Schizophr. Bull. 2014:sbu031.

Gardner DM, Murphy AL, O'Donnell H, Centorrino F, Baldessarini RJ. International Consensus Study of Antipsychotic Dosing. Am J Psychiatry. 2010; 167:686–693. [PubMed: 20360319]

Hadjipapas A, Hillebrand A, Holliday IE, Singh KD, Barnes GR. Assessing interactions of linear and nonlinear neuronal sources using MEG beamformers: a proof of concept. Clin. Neurophysiol. 2005; 116:1300–1313. [PubMed: 15978493]

Hall EL, Woolrich MW, Thomaz CE, Morris PG, Brookes MJ. Using variance information in magnetoencephalography measures of functional connectivity. NeuroImage. 2013; 67:203–212. [PubMed: 23165323]

Hamalainen MS, Sarvas J. Realistic conductivity geometry model of the human head for interpretation of neuromagnetic data. IEEE Trans. Biomed. Eng. 1989; 36:165–171. [PubMed: 2917762]

Hanlon FM, Houck JM, Klimaj Sd, Caprihan A, Mayer AR, Weisend MP, Bustillo JR, Hamilton DA, Tesche CD. Frontotemporal anatomical connectivity and working-relational memory performance predict everyday functioning in schizophrenia. Psychophysiology. 2012; 49:1340–1352. [PubMed: 22882287]

Hanlon FM, Houck JM, Pyeatt CJ, Lundy SL, Euler MJ, Weisend MP, Thoma RJ, Bustillo JR, Miller GA, Tesche CD. Bilateral hippocampal dysfunction in schizophrenia. NeuroImage. 2011; 58:1158–1168. [PubMed: 21763438]

Hillebrand, A.; Barnes, GR. Beamformer Analysis of MEG Data. In: Neurobiology, B-IR., editor. Magnetoencephalography. Academic Press; 2005. p. 149-171.

Himberg, J.; Hyvarinen, A. Icasso: software for investigating the reliability of ICA estimates by clustering and visualization. 2003 IEEE 13th Workshop on Neural Networks for Signal Processing, 2003. NNSP'03; Presented at the 2003 IEEE 13th Workshop on Neural Networks for Signal Processing, 2003. NNSP'03; 2003. p. 259-268.

Hipp JF, Hawellek DJ, Corbetta M, Siegel M, Engel AK. Large-scale cortical correlation structure of spontaneous oscillatory activity. Nat. Neurosci. 2012; 15:884–890. [PubMed: 22561454]

Jafri MJ, Pearlson GD, Stevens M, Calhoun VD. A method for functional network connectivity among spatially independent resting-state components in schizophrenia. NeuroImage. 2008; 39:1666–1681. [PubMed: 18082428]

Jardri R, Pouchet A, Pins D, Thomas P. Cortical Activations During Auditory Verbal Hallucinations in Schizophrenia: A Coordinate-Based Meta-Analysis. Am. J. Psychiatry. 2010; 168:73–81. [PubMed: 20952459]

Jerbi K, Baillet S, Mosher JC, Nolte G, Garnero L, Leahy RM. Localization of realistic cortical activity in MEG using current multipoles. NeuroImage. 2004; 22:779–793. [PubMed: 15193607]

Khadka S, Meda SA, Stevens MC, Glahn DC, Calhoun VD, Sweeney JA, Tamminga CA, Keshavan MS, O'Neil K, Schretlen D, Pearlson GD. Is Aberrant Functional Connectivity A Psychosis Endophenotype? A Resting State Functional Magnetic Resonance Imaging Study. Biol. Psychiatry. 2013; 74:458–466. [PubMed: 23746539]

Kim SG, Richter W, Uğurbil K. Limitations of temporal resolution in functional MRI. Magn. Reson. Med. Off. J. Soc. Magn. Reson. Med. Soc. Magn. Reson. Med. 1997; 37:631–636.

Kiviniemi V, Starck T, Remes J, Long X, Nikkinen J, Haapea M, Veijola J, Moilanen I, Isohanni M, Zang Y-F, Tervonen O. Functional segmentation of the brain cortex using high model order group PICA. Hum. Brain Mapp. 2009; 30:3865–3886. [PubMed: 19507160]

Kolder H, North AW. Oscillations of the Corneo-Retinal Potential in Animals. Ophthalmologica. 1966; 152:149–160. [PubMed: 5965198]

Kühn S, Gallinat J. Resting-State Brain Activity in Schizophrenia and Major Depression: A Quantitative Meta-Analysis. Schizophr. Bull. 2013; 39:358–365. [PubMed: 22080493]

Lee H, Dvorak D, Fenton AA. Targeting Neural Synchrony Deficits is Sufficient to Improve Cognition in a Schizophrenia-Related Neurodevelopmental Model. Front. Psychiatry. 2014:5. [PubMed: 24478733]

Luckhoo H, Hale JR, Stokes MG, Nobre AC, Morris PG, Brookes MJ, Woolrich MW. Inferring task-related networks using independent component analysis in magnetoencephalography. NeuroImage. 2012; 62:530–541. [PubMed: 22569064]

Palva S, Palva JM. Discovering oscillatory interaction networks with M/EEG: challenges and breakthroughs. Trends Cogn. Sci. 2012; 16:219–230. [PubMed: 22440830]

Paterson AS. The Respiratory Rhythm in Normal and Psychotic Subjects. J. Neurol. Psychopathol. 1935; 16:36–53. [PubMed: 21610814]

Piantoni G, Van Der Werf YD, Jensen O, Van Someren EJW. Memory traces of long-range coordinated oscillations in the sleeping human brain. Hum. Brain Mapp. in press. n/a-n/a.

Rachow T, Berger S, Boettger MK, Schulz S, Guinjoan S, Yeragani VK, Voss A, Bär K-J. Nonlinear relationship between electrodermal activity and heart rate variability in patients with acute schizophrenia. Psychophysiology. 2011; 48:1323–1332. [PubMed: 21496056]

Raichle ME, MacLeod AM, Snyder AZ, Powers WJ, Gusnard DA, Shulman GL. A Default Mode of Brain Function. Proc. Natl. Acad. Sci. 2001; 98:676–682. [PubMed: 11209064]

Reeve, A.; Knight, J.; Maclin, E.; Lewine, J.; Orrison, W. Abstracts, International Congress for Schizophrenia Research. Colorado Springs: 1993. Resting-state magnetoencephalography in schizophrenia.

Robinson S, Basso G, Soldati N, Sailer U, Jovicich J, Bruzzone L, Kryspin-Exner I, Bauer H, Moser E. A resting state network in the motor control circuit of the basal ganglia. BMC Neurosci. 2009; 10:137. [PubMed: 19930640]

Rosadini G, Rodriguez G, Siani C. Acute alcohol poisoning in man: An experimental electrophysiological study. Psychopharmacologia. 1974; 35:273–285. [PubMed: 4829325]

Sarvas J. Basic mathematical and electromagnetic concepts of the biomagnetic inverse problem. Phys. Med. Biol. 1987; 32:11. [PubMed: 3823129]

Schoffelen J-M, Gross J. Source connectivity analysis with MEG and EEG. Hum. Brain Mapp. 2009; 30:1857–1865. [PubMed: 19235884]

Scott A, Courtney W, Wood D, de la Garza R, Lane S, King M, Wang R, Roberts J, Turner JA, Calhoun VD. COINS: An Innovative Informatics and Neuroimaging Tool Suite Built for Large Heterogeneous Datasets. Front. Neuroinformatics. 2011; 5:33.

Sehatpour P, Molholm S, Schwartz TH, Mahoney JR, Mehta AD, Javitt DC, Stanton PK, Foxe JJ. A human intracranial study of long-range oscillatory coherence across a frontal–occipital–hippocampal brain network during visual object processing. Proc. Natl. Acad. Sci. 2008; 105:4399–4404. [PubMed: 18334648]

Shostak VI. Reflection of excitability of the visual centers in the spontaneous electroencephalogram in man. Zhurnal Vysshei Nervn. Deyatelnosti. 1968; 18:880–885.

Siebenhühner F, Weiss SA, Coppola R, Weinberger DR, Bassett DS. Intra- and Inter-Frequency Brain Network Structure in Health and Schizophrenia. PLoS ONE. 2013; 8:1–13.

Skouras S, Gray M, Critchley H, Koelsch S. fMRI Scanner Noise Interaction with Affective Neural Processes. PLoS ONE. 2013; 8:e80564. [PubMed: 24260420]

Skudlarski P, Jagannathan K, Anderson K, Stevens MC, Calhoun VD, Skudlarska BA, Pearlson G. Brain Connectivity Is Not Only Lower but Different in Schizophrenia: A Combined Anatomical and Functional Approach. Biol. Psychiatry, Schizophrenia: N-methyl-D-aspartate Receptor Dysfunction and Cortical Connectivity. 2010; 68:61–69.

Sommer IE, Clos M, Meijering AL, Diederen KMJ, Eickhoff SB. Resting State Functional Connectivity in Patients with Chronic Hallucinations. PLoS ONE. 2012; 7:e43516. [PubMed: 22970130]

Stein, A von; Rappelsberger, P.; Sarnthein, J.; Petsche, H. Synchronization Between Temporal and Parietal Cortex During Multimodal Object Processing in Man. Cereb. Cortex. 1999; 9:137–150. [PubMed: 10220226]

Stephan KE, Baldeweg T, Friston KJ. Synaptic Plasticity and Dysconnection in Schizophrenia. Biol. Psychiatry. 2006; 59:929–939. [PubMed: 16427028]

Stephan KE, Friston KJ, Frith CD. Dysconnection in Schizophrenia: From Abnormal Synaptic Plasticity to Failures of Self-monitoring. Schizophr Bull. 2009; 35:509–527. [PubMed: 19155345]

Stone DB, Coffman BA, Bustillo JR, Aine CJ, Stephen JM. Multisensory stimuli elicit altered oscillatory brain responses at gamma frequencies in patients with schizophrenia. Front. Hum. Neurosci. 2014; 8:788. [PubMed: 25414652]

Tallon-Baudry C, Mandon S, Freiwald WA, Kreiter AK. Oscillatory Synchrony in the Monkey Temporal Lobe Correlates with Performance in a Visual Short-term Memory Task. Cereb. Cortex. 2004; 14:713–720. [PubMed: 15054050]

Taulu S, Kajola M. Presentation of electromagnetic multichannel data: The signal space separation method. J. Appl. Phys. 2005; 97:124905–124910.

Thatcher RW, North DM, Biver CJ. Development of cortical connections as measured by EEG coherence and phase delays. Hum. Brain Mapp. 2008; 29:1400–1415. [PubMed: 17957703]

Toichi M, Kubota Y, Murai T, Kamio Y, Sakihama M, Toriuchi T, Inakuma T, Sengoku A, Miyoshi K. The influence of psychotic states on the autonomic nervous system in schizophrenia. Int. J. Psychophysiol. 1999; 31:147–154. [PubMed: 9987060]

Uhlhaas PJ, Singer W. The Development of Neural Synchrony and Large-Scale Cortical Networks During Adolescence: Relevance for the Pathophysiology of Schizophrenia and Neurodevelopmental Hypothesis. Schizophr. Bull. 2011; 37:514–523. [PubMed: 21505118]

Uhlhaas PJ, Singer W. Abnormal neural oscillations and synchrony in schizophrenia. Nat. Rev. Neurosci. 2010; 11:100–113. [PubMed: 20087360]

Uusitalo MA, Ilmoniemi RJ. Signal-space projection method for separating MEG or EEG into components. Med. Biol. Eng. Comput. 1997; 35:135–140. [PubMed: 9136207]

Wens V. Investigating complex networks with inverse models: Analytical aspects of spatial leakage and connectivity estimation. Phys. Rev. E. 2015; 91:12823.

Werner S, Malaspina D, Rabinowitz J. Socioeconomic Status at Birth Is Associated With Risk of Schizophrenia: Population-Based Multilevel Study. Schizophr Bull. 2007; 33:1373–1378. [PubMed: 17443013]

Whitehorn JC, Richter H. Unsteadiness of the heart rate in psychotic and neurotic states. Arch. Neurol. Psychiatry. 1937; 38:62–70.

Wittkower E. Further Studies in the Respiration of Psychotic Patients. Br. J. Psychiatry. 1934; 80:692–704.

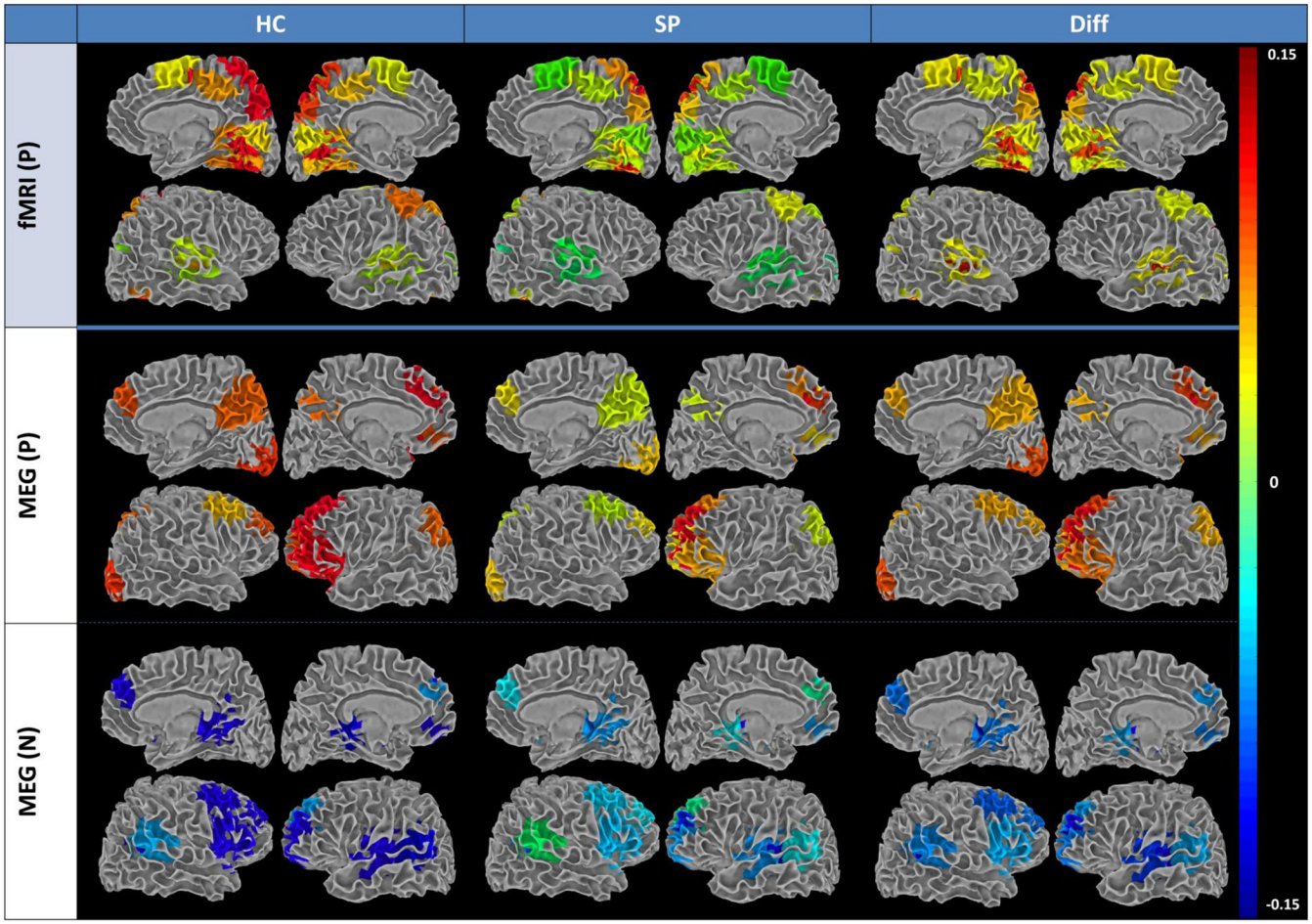

Figure 1.

Summary of functional network connectivity (FNC) group averages and group differences (Healthy Control [HC] - Schizophrenia patient [SZ]) for fMRI and MEG rendered on white matter surface. N = negative (i.e., SZ > HC); P = positive (i.e., HC > SZ). FNC is a measure of among-network connectivity; that is, pairwise correlations in network (ICA component) timecourses. Only those regions involved in significant group differences are included. For networks showing a significant group difference, the rendered values represent the weighted sum of the five strongest correlations with that network.

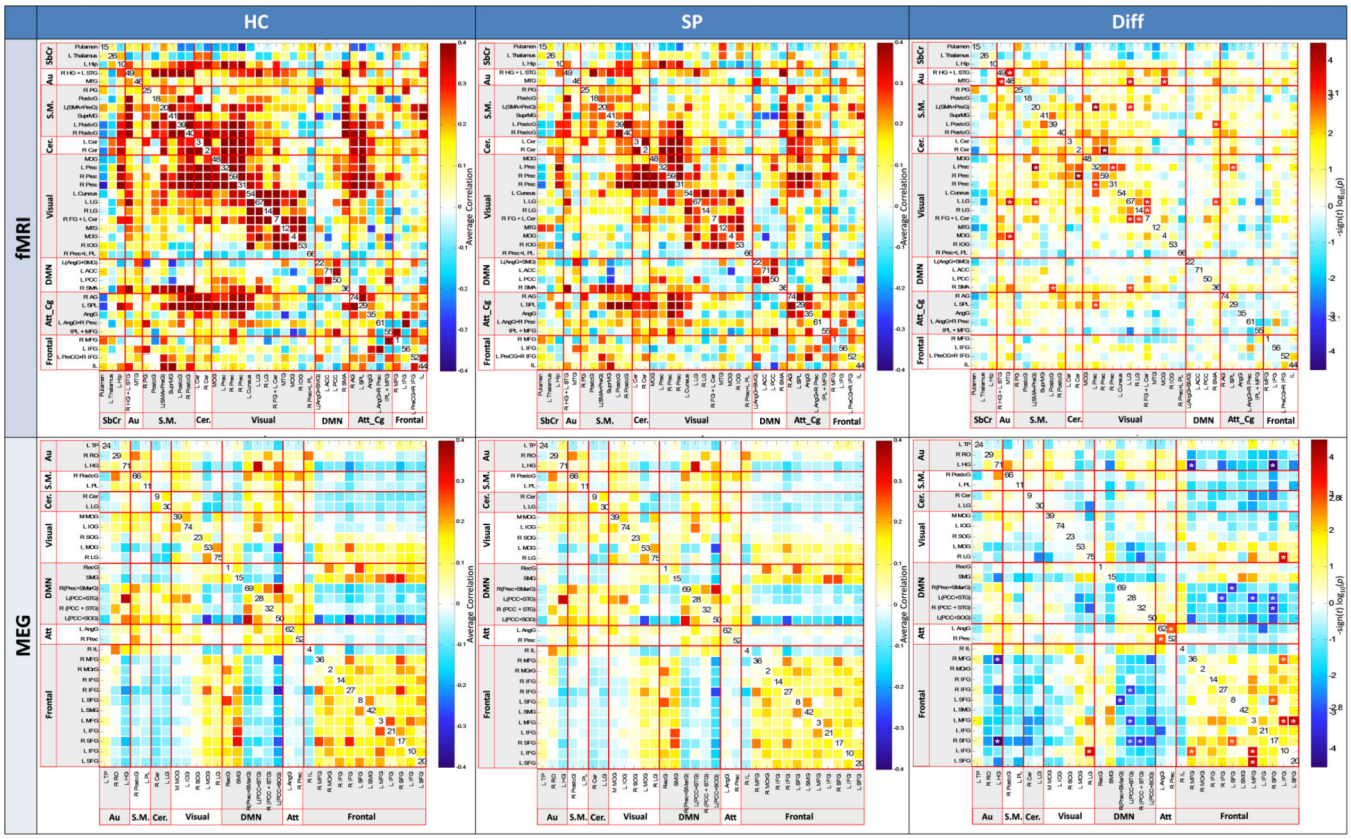

Figure 2.

Functional network connectivity (FNC) for fMRI (top) and MEG (bottom), for healthy controls (left column), Schizophrenia patients (center column), and FDR-corrected group differences (right column). ICA component numbers are on the diagonal. Color scale describes the *p* value after FDR correction.

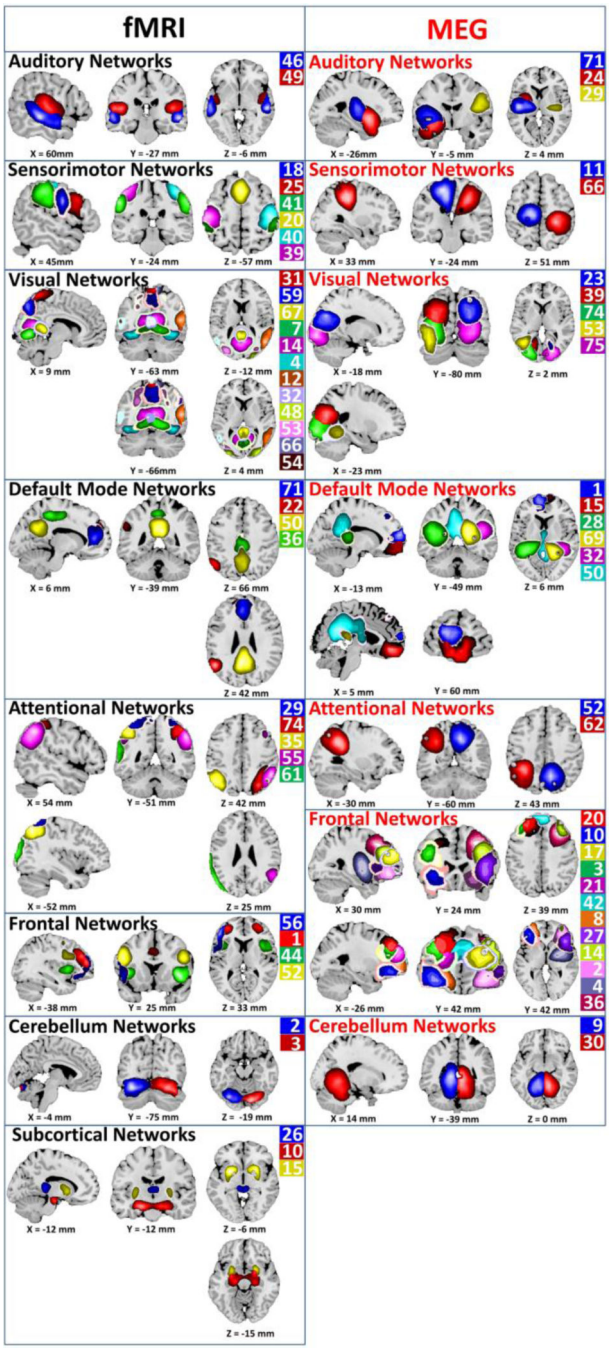

Figure 3.
fMRI and MEG network spatial maps. Color scale is arbitrary and corresponds to the ICA component number.

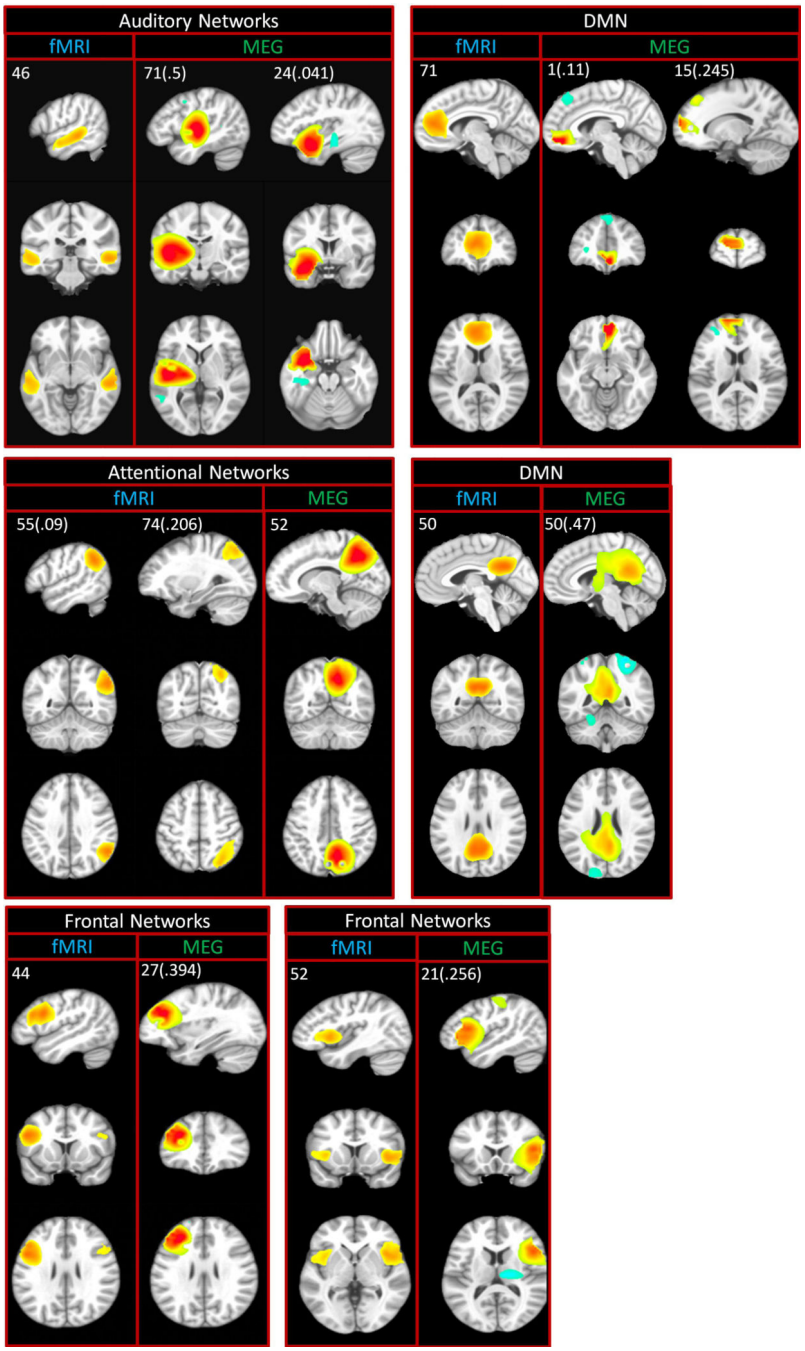

Figure 4.

Spatial overlap in spatial maps (ICA components) detected using MEG and fMRI. ICA component numbers are located in the upper left of each panel. Values in parentheses are the mean spatial correlation between the MEG and corresponding fMRI component. Color scale is *z*-scored component magnitude.

Table 1

Demographic information

	Mean (SD)		*t* or X^2
	Schizophrenia (n=44)	**Control (n=47)**	***(p-value)***
Demographics			
Age	37.28 (13.86)	35.18 (11.83)	0.78 (0.44)
Gender (M/F)	37/7	34/13	0.27 (0.78)
Ethnicity (H/NH)	23/21	26/21	
Race			
American Indian/Alaska Native	2	2	
Asian	2	0	
Black or African American	1	4	
Native Hawaiian or Other Pacific Islander	1	0	
White	38	41	
Socioeconoic status			
Primary caregiver education	4.24 (2.11)	4.53 (1.18)	
Secondary caregiver education	4.72 (1.83)	4.72 (1.84)	
PANSS			
Positive	15.13 (5.136)		
Negative	15.15 (5.013)		
General	29.79 (8.108)		
Medications			
OLZ(mg/day)	14.02 (12.39)		